Journal of Biomedical Optics 9(6), 1129–1136 (November/December 2004)

Intraoperatively assessed optical properties of malignant and healthy breast tissue used to determine the optimum wavelength of contrast for optical mammography

R. L. P. van Veen
H. J. C. M. Sterenborg
Erasmus Medical Center
Daniel den Hoed Cancer Center
Department of Radiation Oncology
Photodynamic Therapy and Optical Spectroscopy Programme
P.O. Box 2040
3008 CA, Rotterdam
The Netherlands
E-mail: h.j.c.m.sterenborg@erasmusmc.nl

A. W. K. S. Marinelli
M. Menke-Pluymers
Erasmus Medical Center
Department of Surgery
Rotterdam, The Netherlands

Abstract. We use spatially resolved diffuse remittance spectroscopy (DRS) for the measurement of absorption (μ_a) and reduced scattering (μ_s') coefficients of normal and malignant breast tissue *in vivo* during surgery. Prior to these measurements, the linearity of the measurement technique was evaluated on liquid optical phantoms. In addition, the reproducibility of *in-vivo* tissue measurements was determined on a healthy volunteer. We present results of the *in-vivo* measurement of optical properties in the wavelength range from 600 to 1100 nm performed during radical mastectomy. A total of 24 patients were included in the study. Both the absorption and reduced scattering properties show large variations. Significant differences in optical properties between normal (glandular plus lipid rich tissue) and tumor tissues are present in 74% of all patients. However, in some cases the tumor showed lower values than normal tissue, and in other cases this was the other way around. Thus, a general trend in optical properties is not observed. However, the average absorption contrast of all patients as a function of wavelength reveals an optimal contrast peak at 650 nm. We believe that this relates to a difference in vascular saturation between tumor and adjacent normal tissue. © *2004 Society of Photo-Optical Instrumentation Engineers.* [DOI: 10.1117/1.1803547]

Keywords: diffuse remittance spectroscopy; absorption coefficent; reduced scattering coefficent; breast tissue; optical mammography.

Paper 94005 received Mar. 2, 2004; revised manuscript received May 19, 2004, and Jun. 21, 2004; accepted for publication Jun. 23, 2004.

1 Introduction

Breast cancer is the most widespread nonskin malignancy among women within the United States and most European countries. In Europe, annual mortality rates are about 70,000. The current standard breast cancer screening tools are palpation and x-ray mammography. However, the latter technique is associated with insufficient specificity, resulting in a large number of false positives. This leads to many unnecessary biopsies and surgical procedures. X-ray mammography depends on the use of ionizing radiation and is of limited use for young women and women with radiographic dense breasts. Furthermore, the use of ionizing radiation comprises the risk of cancer induction. Near-infrared optical imaging is a relatively new nonionizing and noninvasive quantitative technique for the detection of breast cancer. Multispectral near-infrared (NIR) imaging and spectroscopy might provide several advantages, such as low cost compared to CT and MRI. More important, however, is that optical imaging may provide information complementary to currently employed techniques, such as tissue oxygenation levels, total hemoglobin, water, and lipid content, that may improve the contrast between normal, benign, and malignant tissue structures. Currently, several groups are investigating different optical techniques, e.g., tomographic,[1–7] multispectral transillumination,[8–11] optical imaging, or functional spectroscopy techniques,[12–15] either continuous wave, or by time- or frequency-resolved techniques. Spectra or images result from differences in optical properties, i.e., reduced scattering and absorption coefficients, respectively. These result from variations in (extra) cellular refractive indices and oxyhemoglobin, deoxyhemoglobin (oxygenation), water, and lipid chromophore content, respectively. There is evidence in the literature that malignant and benign tissue structures can be discriminated from adjacent normal tissue by their water/lipid ratios, or due to differences in total hemoglobin content and oxygenation, e.g., tumors are associated with an increase in blood volume and a decrease in oxygenation proliferaty.[16,17] Spectral information on reduced scattering coefficients may provide information of scatter center size and density, and is related to the tissue composition and cellular structure. For contrast optimization it is therefore necessary to have detailed spectral knowledge of *in-vivo* optical properties to select the optimal detection wavelengths. As tissue optical properties are

Address all correspondence to Henricus J. C. M. Sterenborg, University Hospital Rotterdam, Dept. of Radiation Oncology, Photodynamic Therapy & Optical Spectroscopy Program, PO Box 5201, NL-3008AE Rotterdam, Netherlands. Tel: 31-10-4391451; Fax: 31-10-439-1012; E-mail: h.j.c.m.sterenborg @erasmusmc.nl

1083-3668/2004/$15.00 © 2004 SPIE

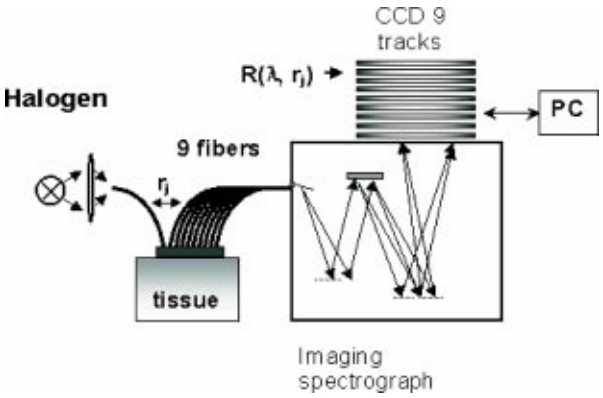

Fig. 1 Basic layout of the diffuse reflectance spectroscopy setup.

strongly influenced by tissue physiology, it is therefore imperative to perform these measurements *in vivo*.

The aim of this study was to determine intrinsic *in-vivo* optical properties of various breast tissue types, e.g., normal glandular tissue, subcutaneous fat, skin, and different malignant tissue pathologies. To do these measurements *in vivo* as close to the target volume as possible, we have performed these measurements intraoperatively. For this we used an optical measurement technique known as spatially resolved diffuse remittance spectroscopy (DRS). This is a relatively simple technique that allows for high-resolution measurement optical properties over a broad wavelength bandwidth.[18,19] Prior to the clinical study, the system linearity was checked by means of liquid tissue phantoms. Furthermore, we determined the reproducibility of the method by means of a series of repeated measurements on a single volunteer.

2 Materials and Methods

2.1 *Experimental Setup*

The setup used is shown schematically in Fig. 1. The illumination of the tissue and the collection of the diffuse re-emitted light are performed by a multifiber probe. This black Perspex probe consists of 10 low hydroxyl (OH^-) medical graded fibers (400-μm core, length approximately 4 m) (CeramOptec GmbH, Bonn, Germany), in which the fibers are positioned at average interfiber distances of 2 mm (2 up to 18 mm). The white light from a 100-W quartz tungsten halogen lamp is coupled into the illumination fiber of the probe. Total light output power of the source fiber was 20 mW. The nine detection fibers in the probe direct the light to the entrance slit position of an imaging spectrograph (Oriel, MS257). The 150-lines/mm grating in the spectrograph allows us to cover a wavelength range from 440 to 1100 nm. A 16-bit 256 to 1024 pixel charge-coupled device (CCD) camera cooled to $-30\,^{\circ}C$ (Andor DU420-OE, Belfast, Northern Ireland) detects the nine reflectance spectra originating at different distances from the illumination fiber.

2.2 *Data Processing*

Data processing and analysis of the data files were performed using custom software written in Matlab (Matlab, Mathworks Incorporated, Massachusetts). The photon propagation in turbid biological tissues can be described using diffusion theory. Farrell, Patterson, and Wilson[20] adapted the diffusion approximation with extrapolated boundary conditions to describe steady-state spatially resolved diffuse reflectance measurements, more recently improved by Kienle and Patterson.[21] In earlier work[19] we used spatially resolved diffuse reflectance spectroscopy for the noninvasive determination of *in-vivo* human tissue optical properties and absolute chromophore concentrations based on this analysis. Rather than calculating optical properties for each of the wavelengths separately, this analysis[18] considered the whole dataset and calculated the absorption and reduced scattering spectra over the entire wavelength range. As a constraint in the analysis, we assumed Lorentz-Mie scattering ($a \cdot \lambda^{-b}$). The diffusion approximation introduces some assumptions into the analysis. The light has to be diffuse, so scattering should dominate absorption. Furthermore, the distance between the source and detector fiber should exceed a minimum distance of approximately $r > 1/\mu_s'$. Based on preliminary results, it was concluded that to satisfy this constraint, the first three fibers had to be excluded from the analysis, consequently the fiber closest to the source was located at a distance of 8 mm.

2.3 *Phantom Measurements*

Prior to the clinical measurements, the linearity of the technique was evaluated on homogeneous liquid optical phantoms[22] using intralipid (Intralipid 20% Fresenius Kabi, Hertogenbosch, Netherlands) and Evans Blue (EB) (ACROS organics, Geel, Belgium). First, the reduced scattering coefficient of the solution was kept constant while increasing the absorption coefficient from 2 m^{-1} up to 10000 m^{-1}. Second, we varied the reduced scattering coefficient while keeping the absorption at a fixed value of 33 m^{-1}. During the measurement, the probe was mechanically held at a fixed position on the phantom surface. The probe was repositioned after each measurement. For each phantom, three measurements were made. Prior to these measurements, the specific absorption coefficient of EB was determined at 630 nm by means of collimated transmission measurements in a scattering-free solution.

2.4 *Volunteer Study*

To investigate reproducibility of *in-vivo* measurements, DRS measurements were performed on a single healthy volunteer (age 26) at ten different locations covering all quadrants in the vicinity of the aureole ($n=5$) and the border of the breast ($n=5$). The fiber optic probe was positioned manually at the measurement site. On each of the ten locations, three sequential measurements were performed without repositioning the probe.

2.5 *Patients*

In this study, 24 patients were enrolled with tumor dimensions exceeding 10 mm. The procedure was performed according to a protocol approved by the local medical ethics committee and with the patient's written informed consent. Histologically confirmed tumors were classified as either 1. benign/reactive, 2. ductal carcinoma in situ (DCIS), or 3. infiltrated; the latter either being of the ductal or lobular adeno type.

During the procedure, the fiber optic probe was placed inside a sterile transparent polyvinyl chloride (PVC) cover

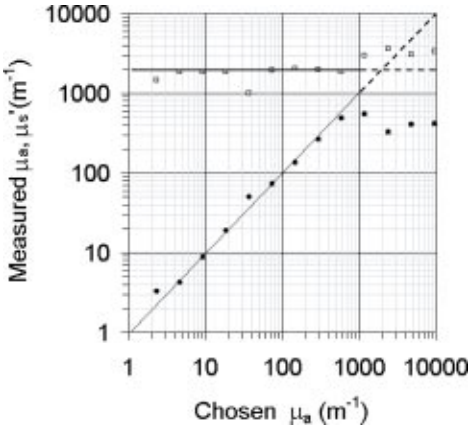

Fig. 2 Absorption and reduced scattering coefficients as measured with DRS versus expected μ_a at constant reduced scattering coefficient ($\mu_s' = 2000\,\mathrm{m}^{-1}$) at λ=630 nm. The dashed line indicates the region where the measured absorption starts to deviate from linearity.

bag (Intercover, International Medical Products, Zutphen, Netherlands). During the measurements, all possible interfering light sources such as the theater lights were turned off and measurements were conducted under subdued light conditions, i.e., less than 50 lux. The fiberoptic probe was held in position manually and placed on the surgical margins of either the tumor or the normal tissue. At each specific tissue location, three sequential measurements were made. If possible, measurements on the same tissue type were taken at several different positions. The total measurement time for a single *in-vivo* measurement was 4 s. Additional surgery time as a result of these measurements was approximately 10 to 15 min. Measurements were performed *in vivo* during modified radical mastectomies with the tissue blood supply still intact. Time of DRS measurements during surgery was halfway through the mastectomy procedure, partially exposing the muscular pectoralis, subcutaneous fat, lipid-rich glandular tissue, and tumor site. In a number of cases, tumors with depths boundaries not lower than 5 mm beneath the skin surface were measured transcutaneously.

3 Results

3.1 *Phantom Study*

Figure 2 shows the results of DRS measurements on the optical phantoms with constant reduced scattering (~2000 m^{-1}) and increasing absorption up to 10000 m^{-1} at 630 nm. The solid straight line represents a linear regression fit through the log values of the data. The slope of the fit was 0.96 and is within the 95% confidence level interval (0.88 to 1.02) with a R^2 value of 0.98. The measured μ_a starts to deviate from the chosen μ_a for $590\,\mathrm{m}^{-1} < \mu_a < 2\,\mathrm{m}^{-1}$, and coupling effects between μ_a and μ_s' are now observed. Figure 3 shows the results of DRS measurements on phantoms with constant absorption of 33 m^{-1} and increasing reduced scattering at 630 nm. The solid straight line represents a linear regression fit. The slope of the fitted linear regression was 0.83 and is within the 95% confidence level interval (0.64 to 1.01) with a R^2 value of 0.82. Both slopes are within 95% confidence interval, indicating the systems linear response for reduced scattering

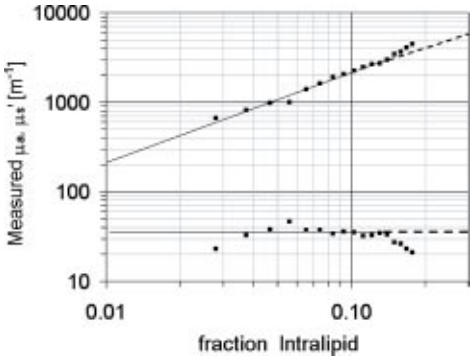

Fig. 3 Scattering coefficients as measured with DRS versus fraction of Intralipid in the phantom solution. Absorption μ_a was kept constant at 33 m^{-1}. The dashed line indicates the region where the measured reduced scattering starts to deviate from linearity.

and absorption. The measured μ_s' starts to deviate from linearity for $\mu_s' > 3000\,\mathrm{m}^{-1}$. The standard deviation originating from repositioning the probe three times is less than 3% for reduced scattering and absorption, respectively.

3.2 *Volunteer*

Figure 4 shows the absorption versus reduced scattering coefficients measured on the volunteer at 900 nm. We calculated the average (μ_a, μ_s'), standard deviation (σ), and relative variation defined as σ/μ of the three sequential measurements at 900 nm for all ten locations (Table 1). Measurements on the same location appeared to reproduce within 4 and 2.6% for absorption and reduced scattering, respectively. Relocating the measurement probe over the ten different locations showed a much larger variability, i.e., 27.2 and 18.6% standard deviation for absorption and reduced scattering, respectively. This large difference suggests that the relative variations within one location reflect the reproducibility of the measurement technique, while the variations between the different locations are due to actual local variations in optical properties within the breast tissue.

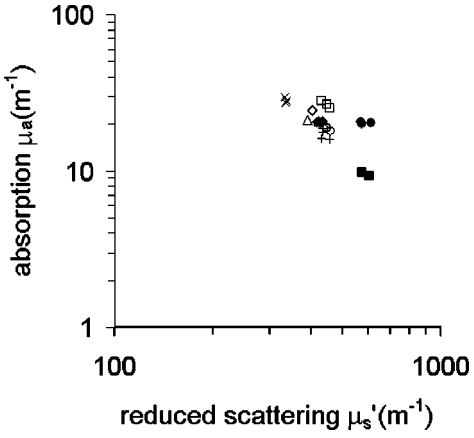

Fig. 4 Absorption versus reduced scattering coefficients at 900 nm measured on the healthy breast of a volunteer. Each group of identical symbols represents three sequential measurements at the same location. Measurements were taken at ten different locations.

Table 1 Analysis of the reproducibility of the measurements at 900 nm. Three repeated measurements on ten locations show that the relative variations between measurements at that same location are roughly 7 times smaller than the relative variations between locations.

Location	μ_a [m^{-1}]	$\sigma/\mu\cdot$ [%]	μ_s' [m^{-1}]	$\sigma/\mu\cdot$ [%]
1	20.6	1.2%	426	1.9%
2	26.7	5.8%	444	3.2%
3	18.5	2.9%	451	1.5%
4	28.4	3.9%	333	0.7%
5	20.7	2.7%	416	5.5%
6	28.0	11.7%	361	2.5%
7	9.6	3.5%	586	3.7%
8	20.3	1.3%	584	4.0%
9	16.5	5.9%	439	3.3%
10	24.5	1.0%	403	0.2%
Mean variation within location	4.0%		2.7%	
Relative variation between locations	27%		19%	

3.3 *Patients*

Intraoperative measurements were performed on 24 patients in total. For each patient, measurements on normal glandular breast tissue could be performed, measured at large distances from the tumor site. In addition, 18 sets of measurements on malignant tissue were made. In six patients, such measurements were not feasible due to either the small size of the tumor, i.e., $<$10 mm ($N=2$, inclusion errors) or the fact that the tumor was too deep below the resection surface (i.e., $>$10 mm). For the normal tissue measurements, the probe was positioned on locations that were visually identified as healthy. Measurements on the palpable tumors were performed at locations where the layer covering the tumor was the thinnest. Three tumors were located only 5 mm below the skin. These tumors were also measured transcutaneously. In total, 312 reliable spectra were recorded. Table 2 gives an overview of the total dataset. Patient age ranged from 37 to 88 years, of which five were premenopausal.

Table 2 Overview of the tissue types measured.

Tissue type measurement	Number of patients
Reactive alteration, hyperplasia	1
DCIS (ductal carcinoma in-situ)	2
Infiltrated lobular/ductal adeno carcinoma	15
Glandular/fat	24
Tumor transcutaneous	3
Muscular pectoralis	10
Breast skin	9

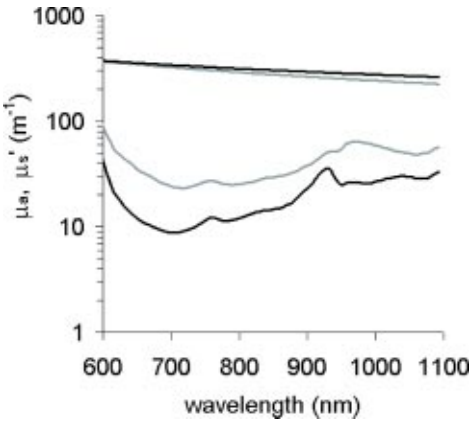

Fig. 5 Example of the *in-vivo* reduced scattering and absorption spectra of normal (black) and malignant (gray) breast tissue versus wavelength in a single patient.

An example of *in-vivo* optical properties of normal and diseased breast tissue in the wavelength range from 600 to 1100 nm is shown in Fig. 5. The age of this patient was 47 and she was premenopausal. The tumor was an infiltrated ductal adeno carcinoma with an average size of 18 mm, located 6 mm underneath the resection surface. For this individual case, the reduced scattering properties did not show any significant differences between tumor and normal. However, a clear and significant difference is seen between the absorption coefficient of the tumor measurement and the measurement performed on normal lipid-rich glandular tissue.

Another individual patient example is shown in Fig. 6. Here absorption is plotted versus reduced scattering at 650 nm for each individual measurement. The age of the patient was 53 and she was postmenopausal. The tumor was a differentiated ductal carcinoma *in situ* after receiving chemotherapy. A student's t-test shows significant differences in absorption be-

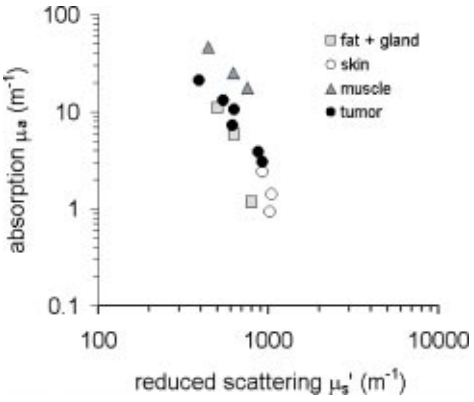

Fig. 6 Example of the absorption plotted versus reduced scattering coefficients at 650 nm for a single patient. Each point represents a single measurement.

Table 3 Fraction of tumors detected for different detection criteria.

Parameter (nm)	Detection score (%)
Scatter power	26.1
μ_s (650)	21.7
μ_s (980)	26.7
μ_a (650)	39.1
μ_a (980)	52.2
Optical penetration depth (650)	39.1
Optical penetration depth (980)	56.5
1-albedo (650)	43.5
1-albedo (980)	39.1
All (650)	52.2
All (980)	69.9
All parameters combined	73.9

tween the means of the normal glandular and tumor tissue measurements ($p<0.05$). No significant differences in reduced scattering between both tissue types are present.

In these two individual cases, the tumors are detectable in optical mammography based on the differences in absorption coefficients between normal and tumor. Such a simple criterion, however, would not be very successful in most other patients.

Tumor detection based on other criteria, i.e., the reduced scattering coefficient, or a combination of absorption, reduced scattering (optical penetration depth, albedo), and scatter power is illustrated in Table 3. Here we list the detection score for different parameter or combination of parameters. The detection score is defined as the percentage of the 18 tumors that is detectable, whereas the detectability of each individual tumor is evaluated by performing a t-test on the means of the specific parameters for tumor and adjacent glandular tissue. In the case of multiple parameters, the tumor is assumed detectable when at least one of the t-tests shows a significant difference. The detection score was calculated from 600 to 1100 nm with a 20-nm interval. Table 3 shows that 74% are detectable at best for a combination of two wavelengths, i.e., 650 and 980 nm. This is not very good, considering all the prior knowledge used.

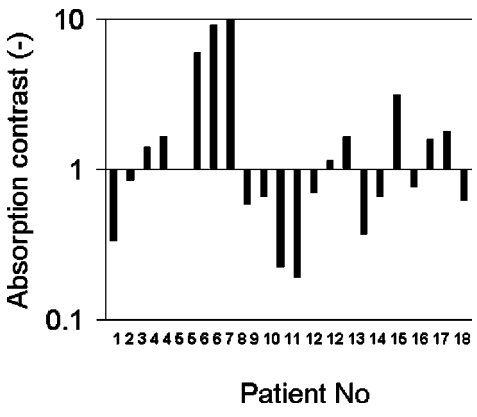

Fig. 7 Absorption contrast between tumor and adjacent lipid-rich glandular tissue calculated for 18 patients at 650 nm.

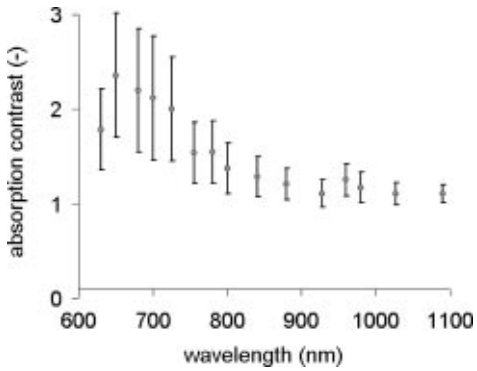

Fig. 8 Average absorption contrast of all patients as a function of wavelength. The error bars represent the standard error of the mean.

Absorption contrast between tumor and adjacent normal (lipid-rich glandular) tissue was calculated for 18 patients by dividing the average of all tumor measurements by the average of all normal measurements in a single patient. Figure 7 shows the absorption contrast at 650 nm for 18 patients. No systematic patterns could be observed, i.e., in some cases (12 out of 22), absorption was higher in tumor than in normal tissue, while in others the opposite was the case. Likewise for scattering, sometimes the tumor showed higher scattering than the adjacent normal glandular tissue, while sometimes it was lower. However, the average absorption contrast of all patients as a function of wavelength revealed a peak at 650 nm with a maximum of 2.4, as depicted in Fig. 8. The error bars given here represent the standard error of the mean, as the standard deviation was very high, as described earlier. Reduced scattering did not reveal any spectral features in contrast, as seen in Fig. 9, and was on average a factor 1.08.

In Fig. 10, the average optical properties of all patients and tissue types at 650 nm are shown, demonstrating overlap be-

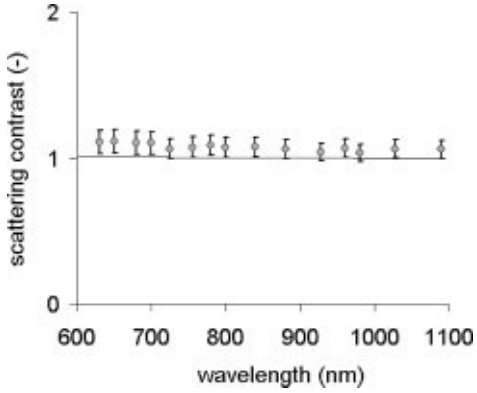

Fig. 9 Average reduced scattering contrast of all patients as a function of wavelength. The error bars represent the standard error of the mean.

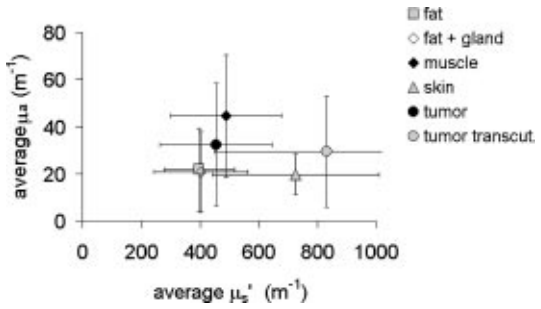

Fig. 10 Average absorption coefficients versus average reduced scattering coefficients of all patients and tissue types at 650 nm. The error bars represent the standard deviation.

tween the different tissue types due to the large standard deviations. However, Fig. 10 confirms the systematic differences between tumor and adjacent glandular tissue.

Values for average Mie scatter power were −0.7 standard deviation (SD) 0.4 for lipid-rich glandular tissue, −1.4 SD 0.5 for muscle, −1.4 SD 0.8 for breast skin, −0.8 SD 0.4 for tumor, and 1.1 SD 0.9 for tumor transcutaneous.

4 Discussion

We present, to our knowledge, the first intraoperatively assessed *in-vivo* optical properties of normal and malignant female breast tissue in the wavelength region between 600 and 1100 nm. In this study large variations in optical properties were observed within subjects, and was even larger over the entire patient group. The DRS method was first tested on a series of homogeneous optical phantoms with the probe fixed on top of the surface. The derived μ_s' were well linear with increasing intralipid concentration, and measured μ_a in good agreement with the predicted absorption, thus demonstrating the methods validity. The scattering properties of Intralipid measured by spatially resolved DRS are comparable with those reported by van Staveren et al.,[22] e.g., 0.1 fraction of Intralipid 20% corresponds to a reduced scattering coefficient of ~2000 m^{-1}. In other studies, spatially resolved DRS was compared with time-resolved DRS by measurement on the same epoxy phantom[23] and pure mammalian lipid sample,[24] and results were in good agreement.

The volunteer measurements showed variations on the order of 4% within a single location. It is unlikely that these variations are related to movement of the manually held fiber optic probe. The sampled volume is several millimeters in diameter, hence only a substantial (i.e., 1 mm or more) movement is expected to cause a substantial change in the sample volumes. More important may be the effect of probe pressure. Increased pressure may push the main absorber, hemoglobin, out of the capillaries and could decrease water concentration due to interstitial water transport,[25] thus altering the optical properties. To a lesser extent, slight changes in probe angle may explain the variations. Repositioning the probe to other locations on the same breast showed even larger variations (27 and 19%), clearly demonstrating large variation in local optical properties.

The intraoperative measurements demonstrated large variations in optical properties, and no strong systematic differences between tumor and normal tissue were observed. Possible differences in optical properties observed may have been diluted to a certain extent because of the presence of a margin of normal tissue on top of the surgically exposed tumor. Measurements directly on the tumor were not possible, as the excision margins around the tumor are between 4 and 15 mm. In principle, the maximum information density of the measured signals is reached around 5 mm in depth, hence we rejected four cases where the resection margin was obviously more than 10 mm. This, however, was based on the surgeon's feeling during surgery and may not have been 100% accurate.

The manual positioning of the fiber optic probe, making good optical contact to the tissue and holding it steady during surgery, proved to be cumbersome, especially in certain locations. Although ambient lights were low, some spectra showed artifacts related to ambient light. This nearly always caused the fit procedure, which was used to transform reflection spectra to optical properties, to become unstable. This occurred in 129 out of the 441 measured spectra. Some of these cases were identifiable by the ambient light artifacts, but most were related to bad optical contact. We believe that some of the failures that produced an unstable fit were related to inhomogeneities in the tissue in the measurement volume, such as large blood vessels. The mathematical models used to analyze the data assume a homogenous medium. Volumes probed with the DRS technique are between 0.1 and 2 cm^3. Inhomogeneities within such a volume can easily occur, producing a mathematical incompatibility between measurement and model.

Many authors reported breast tissue optical properties either *ex vivo*[26–29] or *in vivo*,[30–32] all demonstrating a large variety in results. In part this can be accounted for by differences in methodology, e.g., *ex-vivo* tissue samples suffer from blood loss and preparation may alter reduced scattering properties. Furthermore, the breast is an inhomogeneous organ consisting of different tissue types, and thus the measurement geometry potentially has a large impact on the *in-vivo* optical properties obtained. In addition, physiological temporal variations such as age-depended breast parenchyma and menstrual cycle[33] have demonstrated to induce large variations in optical properties between pre- and postmenopausal subjects,[34,35] resulting from atrophy of glandular tissue and decrease in water content. Hormone replacement treatment (HRT) is of influence as well and is associated with epithelial proliferation in the ductal tracts and increased water content. Moreover, the different techniques used may be influenced differently by the inhomogeneities mentioned earlier. In the case of a small inhomogeneity that would not cause our fit algorithm to fail, our dc measurement would favor the areas of lowest optical properties, as these would have the largest contribution to the signals. Time resolved late gate measurements, on the other hand, could favor the areas with the largest scattering, as these photons would take longer.

The results of our transcutaneaous measurements coincide with previous work by Shah et al.[15] and Durduran et al.[31] Direct comparison of our intraoperatively measured values is not possible. Tomographically derived optical properties of normal glandular tissue presented by Jiang et al.[7] give higher scattering and lower absorption.

We found a moderately higher detectability in the region where blood absorption is large and near the water peak. The average contrast of all patients as a function of wavelength revealed an optimal contrast peak at 650 nm that can be re-

lated to a systematic difference in blood oxygenation between tumor and adjacent normal tissue. The ratio, as seen in Fig. 8, could be explained by a drop in blood saturation from 90% in normal tissue to 55% in and around the tumor. A similar trend in contrast between tumor and normal breast tissue has recently been demonstrated by Taroni et al.[36]

Although promising results are demonstrated in several ongoing trials, e.g., Refs. 37 and 38, there is still unsatisfactory results with regard to the sensitivity for detection of fairly large tumors. These results are confirmed in the present study. Although the optical imaging technique in itself may be very powerful, its diagnostic success relies on the presence of a contrast between tumor and normal. Based on the present findings, it is suggested that optimal contrast could be found around 650 nm, i.e., the wavelength region most sensitive to differences in tissue oxygenation.

5 Conclusion

The optical properties of different breast tissues are measured in the spectral range from 600 to 1100 nm, demonstrating large intra- and inter-patient variations. We believe that these variations are mainly due the heterogeneous nature of breast tissue, consequently this resulted in large differences in local optical properties partially masking possible differences between tumor and normal. Additional variations are introduced by tissue inhomogeneities and measurement artifacts, e.g., ambient light and probe tissue contact, e.g., misalignment of the sterile clear cover material and probe pressure. In 74% of the cases, the tumor could be distinguished from its surrounding normal tissue on the basis of significant difference of the average optical properties. However, no systematic differences are observed between tumor and normal tissue. In cases where significant differences are observed between tumor and adjacent normal tissue, we saw no systematic behavior, i.e., scattering as well as absorption of tumor tissue could either be higher or lower than normal tissue. However, the average absorption contrast of all patients as a function of wavelength revealed an optimal contrast peak at 650 nm that can be related to a difference in tissue oxygenation between tumor and adjacent normal tissue.

Acknowledgments

The work was partially supported by the European Union Project Optimamm (contract QLG1-CT-2000-00690). Contract QLG1-2000-01464 from the European Union Network Medphot is also acknowledged.

References

1. J. C. Hebden, H. Veenstra, H. Dehghani, E. M. Hillman, M. Schweiger, S. R. Arridge, and D. T. Delpy, ''Three-dimensional time-resolved optical tomography of a conical breast phantom,'' *Appl. Opt.* **40**, 3278–3287 (2001).
2. B. W. Pogue, S. P. Poplack, T. O. McBride, W. A. Wells, K. S. Osterman, U. L. Osterberg, and K. D. Paulsen, ''Quantitative hemoglobin tomography with diffuse near-infrared spectroscopy: pilot results in the breast,'' *Radiology* **218**, 261–266 (2001).
3. Q. Zhu, M. Huang, N. Chen, K. Zarfos, B. Jagjivan, M. Kane, P. Hedge, and S. H. Kurtzman, ''Ultrasound-guided optical tomographic imaging of malignant and benign breast lesions: initial clinical results of 19 cases,'' *Neoplasia* **5**, 379–388 (2003).
4. J. P. Culver, R. Choe, M. J. Holboke, L. Zubkov, T. Durduran, A. Slemp, V. Ntziachristos, B. Chance, and A. G. Yodh, ''Three-dimensional diffuse optical tomography in the parallel plane transmission geometry: evaluation of a hybrid frequency domain/continuous wave clinical system for breast imaging,'' *Med. Phys.* **30**, 235–247 (2003).
5. A. Li, E. L. Miller, M. E. Kilmer, T. J. Brukilacchio, T. Chaves, J. Stott, Q. Zhang, T. Wu, M. Chorlton, R. H. Moore, D. B. Kopans, and D. A. Boas, ''Tomographic optical breast imaging guided by three-dimensional mammography,'' *Appl. Opt.* **42**, 5181–5190 (2003).
6. S. Srinivasan, B. W. Pogue, S. Jiang, H. Dehghani, C. Kogel, S. Soho, J. J. Gibson, T. D. Tosteson, S. P. Poplack, and K. D. Paulsen, ''Interpreting hemoglobin and water concentration, oxygen saturation, and scattering measured in vivo by near-infrared breast tomography,'' *Proc. Natl. Acad. Sci. U.S.A.* **100**, 12349–12354 (2003).
7. H. Jiang, N. V. Iftimia, Y. Xu, J. A. Eggert, L. L. Fajardo, and K. L. Klove, ''Near-infrared optical imaging of the breast with model-based reconstruction,'' *Acad. Radiol.* **9**, 186–194 (2002).
8. A. Pifferi, P. Taroni, A. Torricelli, F. Messina, R. Cubeddu, and G. Danesini, ''Four-wavelength time-resolved optical mammography in the 680–980-nm range,'' *Opt. Lett.* **28**, 1138–1140 (2003).
9. D. Grosenick, K. T. Moesta, H. Wabnitz, J. Mucke, C. Stroszczynski, R. Macdonald, P. M. Schlag, and H. Rinneberg, ''Time-domain optical mammography: initial clinical results on detection and characterization of breast tumors,'' *Appl. Opt.* **42**, 3170–3186 (2003).
10. S. Fantini, S. Walker, M. A. Franceschini, M. Kaschke, P. M. Schlag, and K. T. Moesta, ''Assesment of size, position and optical properties of breast tumors in vivo by nonivasive optical methods,'' *Appl. Opt.* **37**, 1982–1989 (1998).
11. M. A. Franceschini, K. T. Moesta, S. Fantini, G. Gaida, E. Gratton, H. Jess, W. W. Mantulin, M. Seeber, P. M. Schlag, and M. Kaschke, ''Frequency-domain techniques enhance optical mammography: initial clinical results,'' *Proc. Natl. Acad. Sci. U.S.A.* **94**, 6468–6473 (1997).
12. B. J. Tromberg, O. Coquoz, J. B. Fishkin, T. Pham, E. R. Anderson, J. Butler, M. Cahn, J. D. Gross, V. Venugopalan, and D. Pham, ''Non-invasive measurements of breast tissue optical properties using frequency-domain photon migration,'' *Philos. Trans. R. Soc. London, Ser. B* **352**, 661–668 (1997).
13. B. J. Tromberg, N. Shah, R. Lanning, A. Cerussi, J. Espinoza, T. Pham, L. Svaasand, and J. Butler, ''Non-invasive in vivo characterization of breast tumors using photon migration spectroscopy,'' *Neoplasia* **2**, 26–40 (2000).
14. A. E. Cerussi, D. Jakubowski, N. Shah, F. Bevilacqua, R. Lanning, A. J. Berger, D. Hsiang, J. Butler, R. F. Holcombe, and B. J. Tromberg, ''Spectroscopy enhances the information content of optical mammography,'' *J. Biomed. Opt.* **7**, 60–71 (2002).
15. N. Shah, A. Cerussi, C. Eker, J. Espinoza, J. Butler, J. Fishkin, R. Hornung, and B. Tromberg, ''Noninvasive functional optical spectroscopy of human breast tissue,'' *Proc. Natl. Acad. Sci. U.S.A.* **98**, 4420–4425 (2001).
16. S. Thomsen and D. Tatman, ''Physiological and pathological factors of human breast disease that can influence optical diagnosis,'' *Ann. N.Y. Acad. Sci.* **838**, 171–193 (1998).
17. B. Beauvoit, T. Kitai, and B. Chance, ''Contribution of the mitochondrial compartment to the optical properties of the rat liver: a theoretical and practical approach,'' *Biophys. J.* **67**, 2501–2510 (1994).
18. R. L. P. van Veen, W. Verkruijsse, and H. J. C. M. Sterenborg, ''Diffuse reflectance spectroscopy from 500 to 1060 nm by correction for inhomogenously distributed absorbers,'' *Opt. Lett.* **27**, 246–248 (2002).
19. R. M. P. Doornbos, R. Lang, F. W. Cross, and H. J. C. M. Sterenborg, ''The determination of in-vivo human tissue optical properties and absolute chromophore concentrations using spatially resolved steady state diffuse reflectance spectroscopy,'' *Phys. Med. Biol.* **44**, 967–981 (1999).
20. T. J. Farrell, M. S. Patterson, and B. Wilson, ''A diffusion theory model of spatially resolved, steady-state diffuse reflectance for the noninvasive determination of tissue optical properties in vivo,'' *Med. Phys.* **19**, 879–888 (1992).
21. A. Kienle and M. S. Patterson, ''Improved solutions of the steady-state and the time-resolved diffusion equations for reflectance from a semi-infinite turbid medium,'' *J. Opt. Soc. Am. A* **14**, 246–254 (1997).
22. H. J. van Staveren, C. J. M. Moes, J. van Marle, S. A. Prahl, and M. J. C. van Gemert, ''Light scattering in Intralipid 10% in the wavelength region of 400–1100 nm,'' *Appl. Opt.* **30**, 4507–4513 (1991).
23. A. Pifferi, A. Torricelli, A. Bassi, P. Taroni, R. Cubeddu, H. Wabnitz, D. Grosenick, M. Möller, R. Macdonald, J. Swartling, T. Svensson, S.

Andersson-Engels, R. L. P. van Veen, H. J. C. M. Sterenborg, J. M. Tualle, E. Tinet, S. Avrillier, M. Whelan, and H. Stamm, ''Performance assessment of photon migration instruments: the Medphot protocol,'' in Biomedical Topical Meetings on CD-ROM, Paper WD7, Optical Society of America, Washington, DC (2004).
24. R. L. P. van Veen, H. J. C. M. Sterenborg, A. Pifferi, A. Torricelli, and R. Cubeddu, ''Determination of VIS- NIR absorption coefficients of mammalian fat, with time- and spatially resolved diffuse reflectance and transmission spectroscopy,'' in Biomedical Topical Meetings on CD-ROM, Paper SF5, Optical Society of America, Washington, DC (2004).
25. S. Jiang, B. W. Pogue, K. D. Paulsen, C. Kogel, and S. P. Poplack, ''In vivo near-infrared spectral detection of pressure-induced changes in breast tissue,'' *Opt. Lett.* **28**, 1212–1214 (2003).
26. T. L. Troy, D. L. Page, and E. M. Sevick-Muraca, ''Optical properties of normal and diseased breast tissues: Prognosis for optical mammography,'' *J. Biomed. Opt.* **1**, 342–355 (1996).
27. V. G. Peters, D. R. Wyman, M. S. Patterson, and G. L. Frank, ''Optical properties of normal and diseased human breast tissues in the visible and near infrared,'' *Phys. Med. Biol.* **35**, 1317–1334 (1990).
28. N. Ghosh, S. Mohanty, S. Majumder, and P. Gupta, ''Measurement of optical properties of normal and malignant human breast tissue,'' *Appl. Opt.* **40**, 176–184 (2001).
29. G. Zacharakis, A. Zolindaki, V. Sakkalis, G. Filippidis, T. G. Papazoglou, D. D. Tsiftsis, and E. Koumantakis, ''In vitro optical characterization and discrimination of female breast tissue during near infrared femtosecond laser pulses propagation,'' *J. Biomed. Opt.* **6**, 446–449 (2001).
30. H. Heusmann, J. Kolzer, and G. Mitic, ''Characterization of female breast in vivo by time resolved and spectroscopic measurements in near infrared spectroscopy,'' *J. Biomed. Opt.* **1**, 425–434 (1996).
31. T. Durduran, R. Choe, J. P. Culver, L. Zubkov, M. J. Holboke, J. Giammarco, B. Chance, and A. G. Yodh, ''Bulk optical properties of healthy female breast tissue,'' *Phys. Med. Biol.* **47**, 2847–2861 (2002).
32. V. Quaresima, S. J. Matcher, and M. Ferrari, ''Identification and quantification of intrinsic optical contrast for near-infrared mammography,'' *Photochem. Photobiol.* **67**, 4–14 (1998).
33. R. Cubeddu, C. D'Andrea, A. Pifferi, P. Taroni, A. Torricelli, and G. Valentini, ''Effects of the menstrual cycle on the red and near-infrared optical properties of the human breast,'' *Photochem. Photobiol.* **72**, 383–391 (2000).
34. B. Chance, ''Near-infrared (NIR) optical spectroscopy characterizes breast tissue hormonal and age status,'' *Acad. Radiol.* **8**, 209–210 (2001).
35. A. E. Cerussi, A. J. Berger, F. Bevilacqua, N. Shah, D. Jakubowski, J. Butler, R. F. Holcombe, and B. J. Tromberg, ''Sources of absorption and scattering contrast for near-infrared optical mammography,'' *Acad. Radiol.* **8**, 211–218 (2001).
36. P. Taroni, A. Pifferi, A. Torricelli, L. Spinelli, G. M. Danesini, and R. Cubeddu, ''Do shorter wavelengths improve contrast in optical mammography?'' *Phys. Med. Biol.* **49**, 1203–1215 (2004).
37. A. Torricelli, L. Spinelli, A. Pifferi, P. Taroni, and R. Cubeddu, ''Use of nonlinear perturbation approach for in-vivo breast lesion characterization by multi-wavelength time-resolved optical mammography,'' *Opt. Express* **11**, 853–867 (2003).
38. D. Grosenick, H. Wabnitz, H. Rinneberg, K. T. Moesta, and P. M. Schlag, ''Development of a time-domain optical mammograph and first in vivo applications,'' *Appl. Opt.* **38**, 2927–2943 (1999).